FRONTIERS OF PHYSICS

RESEARCH ARTICLE
Volume 19 / Issue 3 / 31202 / 2024

General properties of the spectral form factor in open quantum systems

Yi-Neng Zhou[1], Tian-Gang Zhou[1], Pengfei Zhang[2,†]

1 Institute for Advanced Study, Tsinghua University, Beijing 100084, China
2 Department of Physics, Fudan University, Shanghai 200438, China
Corresponding author. E-mail: †PengfeiZhang.physics@gmail.com
Received November 30, 2023; accepted March 25, 2024

ABSTRACT

The spectral form factor (SFF) can probe the eigenvalue statistic at different energy scales as its time variable varies. In closed quantum chaotic systems, the SFF exhibits a universal *dip-ramp-plateau* behavior, which reflects the spectrum rigidity of the Hamiltonian. In this work, we explore the general properties of SFF in open quantum systems. We find that in open systems the SFF first decays exponentially, followed by a linear increase at some intermediate time scale, and finally decreases to a saturated plateau value. We derive general relations between (i) the early-time decay exponent and Lindblad operators; (ii) the long-time plateau value and the number of steady states. We also explain the effective field theory perspective of general behaviors. We verify our theoretical predictions by numerically simulating the Sachdev–Ye–Kitaev (SYK) model, random matrix theory (RMT), and the Bose–Hubbard model.

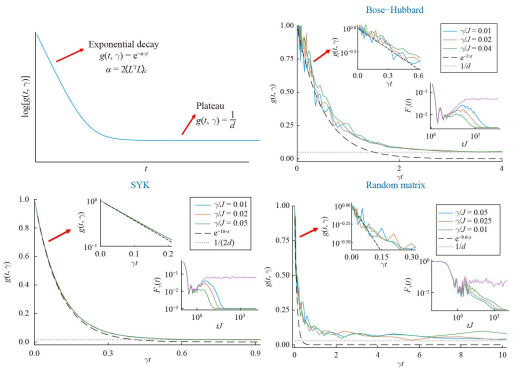

Keywords spectral form factor, open quantum system, quantum chaos

1 Introduction

The spectral form factor (SFF) has attracted much attention in recent years for its direct relation to the eigenvalue statistics at different energy scales and its utility as a robust diagnosis of quantum chaos [1–13]. The structure of SFF is a direct indicator of the energy spectrum correlation in quantum systems. As its time variable increases, it reveals the eigenvalue statistics at a smaller energy scale. The SFF among different models reveals the symmetry that those models preserve. It exhibits several universal properties including the initial decay, the increase at intermediate time scales which shows a linear ramp in models with spectrum rigidity, and finally the saturation to a plateau value. This *dip-ramp-plateau* structure is ubiquitous in quantum chaos systems [14–17].

However, the interaction and exchange between the system and environment are inevitable, and therefore it is natural to focus on the corresponding problem in open systems. Generalizing familiar concepts in closed systems to open systems has helped people discover much more interesting and novel physics. Recently, the development of entropy dynamics [18], entanglement phase transition [19–46], and operator complexity [47–50] in open quantum many-body systems have aroused much interest in condensed matter physicists. Also, there are explorations on the definitions and physical interpretations of the SFF in open systems or non-Hermitian Hamiltonians [51–58].

In this paper, we study the SFF in open quantum systems driven by the Lindblad master equation. The definition we use excludes possible exponential growth over time in general non-Hermitian systems [59]. For concreteness, we define the normalized SFF as the ratio between SFF with dissipation and that without dissipation. We find some general properties of the normalized

Higher Education Press

https://doi.org/10.1007/s11467-024-1406-7

SFF according to its early-time and late-time dynamics. More specifically, we find this normalized SFF has an early-time exponential decay behavior related to the Lindblad operators and late-time plateau behavior related to the number of steady states. We demonstrate the generality of these properties in open systems by studying three different models with dissipation: the random matrix model, the SYK model, and the Bose–Hubbard model. In the random matrix model and the Bose–Hubbard model, the numerical results agree well with our conjecture. Furthermore, using the path-integral method, we give a candidate semi-classical explanation of the SFF in systems with dissipation, and this is a novel perspective for understanding the general properties of the normalized SFF.

2 The definition of SFF in open systems

In the closed system, the SFF can be defined as the size fluctuation of the analytic continuation of the thermal partition function of the quantum system

$$F(t,\beta=0)=\frac{|\mathcal{Z}(\mathrm{i}t)|^2}{[\mathcal{Z}(0)]^2}=\frac{1}{[\mathcal{Z}(0)]^2}\sum_{m,n}\mathrm{e}^{-\mathrm{i}(E_m-E_n)t}, \quad (1)$$

with $\mathcal{Z}(\mathrm{i}t)=\mathrm{Tr}(\mathrm{e}^{-\mathrm{i}tH})$. From this expression, we see that SFF captures the energy level correlations of the full spectrum of the system, and the energy scale that it probes decreases as its time variable increases. At early time, SFF captures the energy level correlations at an energy scale much larger than the mean energy level spacing of the system, and it usually has a decay behavior, often called *slope*. This slope region is non-universal in different models for it sees the details of the energy spectrum of the system. However, it can be universally bounded, regardless of whether the system is chaotic or not [60]. At the intermediate time scale, SFF measures the energy level correlation in the same order as the mean energy level spacing, and in some models that have level repulsion, we see a linear ramp of SFF as time increases. Therefore, SFF can be used to diagnose spectral rigidity. A detailed study of the SFF in terms of spectral distances helps understand this ramp and the transition to the plateau [17]. Over a long time, the SFF often saturates to a constant plateau value determined by each single energy level. Also, there are some studies about the non-universal properties of the form factor in chaotic systems [61, 62].

In the open system, we consider the time evolution of the system driven by the Lindblad Master equation

$$\frac{\partial\hat{\rho}}{\partial t}=-\mathrm{i}[\hat{H},\hat{\rho}]+2\gamma\sum_m\hat{L}_m\hat{\rho}\hat{L}_m^\dagger-\gamma\sum_m\{\hat{L}_m^\dagger\hat{L}_m,\hat{\rho}\}. \quad (2)$$

Here, γ is the dissipation strength, and $\hat{L}_\alpha$ is the Lindblad jump operator. If we use the Choi–Jamiolkwski isomorphism [63, 64] to map the density matrix $\hat{\rho}=\sum_{m,n}\rho_{mn}|m\rangle\langle n|$ to a wave function defined on a doubled space as $|\psi_\rho^D(t)\rangle=\sum_{mn}\rho_{mn}|m\rangle_L\otimes|n\rangle_R$, then after this mapping the wave function ψ_ρ^D in the doubled system satisfies a Schrodinger-like equation $\mathrm{i}\partial_t\psi_\rho^D(t)=\hat{H}^D\psi_\rho^D(t)$. Here, $\hat{H}^D=\hat{H}_s-\mathrm{i}\hat{H}_d$ is defined on the doubled space with

$$\begin{aligned}\hat{H}_s&=\hat{H}_L\otimes\hat{\mathcal{I}}_R-\hat{\mathcal{I}}_L\otimes\hat{H}_R^{\mathrm{T}},\\ \hat{H}_d&=\gamma\sum_m[-2\hat{L}_{m,L}\otimes\hat{L}_{m,R}^*\\ &\quad+(\hat{L}_m^\dagger\hat{L}_m)_L\otimes\hat{\mathcal{I}}_R+\hat{\mathcal{I}}_L\otimes(\hat{L}_m^\dagger\hat{L}_m)_R^*].\end{aligned} \quad (3)$$

Operators with subscripts L and R stand for operators acting on the left and the right systems respectively, "T" stands for the transpose, and $\hat{\mathcal{I}}$ represents the identity operator. Here, both $\hat{H}_L$ and $\hat{H}_R$ take the same form as the original Hamiltonian H, although they act on different Hilbert spaces.

Similar to the SFF defined in the closed system in Eq. (1), we can define the SFF in the open system as

$$F_\gamma(t)=\frac{1}{[\mathcal{Z}(0)]^2}\mathrm{Tr}(\mathrm{e}^{-\mathrm{i}\hat{H}^Dt})=\frac{1}{[\mathcal{Z}(0)]^2}\sum_l\mathrm{e}^{(-\mathrm{i}\alpha_l-\beta_l)t}. \quad (4)$$

Here, we use the subscript γ to denote the SFF in open systems (that is the dissipation strength γ is non-zero). Also, we consider that this non-Hermitian Hamiltonian $\hat{H}^D$ can be diagonalized, yielding a set of eigenstates denoted as $\{\epsilon_l\}$. We represent them as $\epsilon_l=\alpha_l-\mathrm{i}\beta_l$ which provides the second equality in Eq. (4). This spectrum originates from the Lindblad equation and is referred to as the *Lindblad spectrum*. When we set the dissipation strength in the Lindblad evolution as zero, we find that this definition is the same as that in the closed system Eq. (1). Our generalization to open quantum systems is consistent with the definition presented in Can's work [51], referred to as the *dissipative form factor*. In Ref. [51], the primary focus is on Lindbladian terms with randomness, whereas our arguments remain valid for Lindbladian terms without randomness.

Since the imaginary part of the Lindblad spectrum is always non-negative, this SFF defined in Eq. (4) will not grow exponentially. Thus, although the Lindblad spectrum is complex, the SFF defined in Eq. (4) will decay exponentially in time till it reaches the steady state value. In addition, there is an alternative approach to defining the SFF in open systems that has a close relation to the definition Eq. (4), and the details of this discussion are included in the supplementary materials [65].

3 The general function of the normalized SFF

Let us now consider the behavior of the normalized SFF

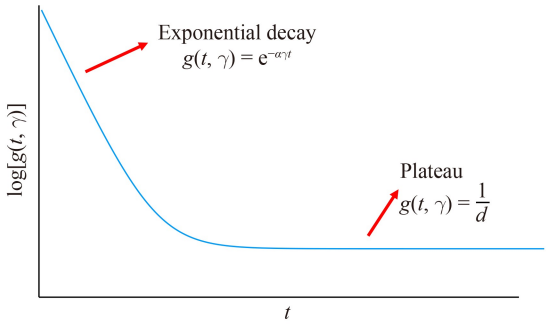

Fig. 1 The general properties of the normalized SFF in open systems. It has an early-time exponential decay and a long-time plateau behavior.

in open systems defined as

$$g(t,\gamma)\equiv\frac{F_\gamma(t)}{F(t,\beta=0)}. \tag{5}$$

The motivation here is to find some general properties of this normalized SFF. We summarize some general properties of this normalized SFF including the early-time exponential decay behavior related to the Lindblad operators and the late-time plateau behavior related to the number of the steady state, and it is illustrated in Fig. 1. We summarize these general properties below.

1) At the early time $\gamma t\ll 1$, the normalized SFF has an exponential decay behavior

$$g(t,\gamma)=e^{-\alpha\gamma t}\quad\text{with }\alpha=\sum_m 2\langle\hat{L}_m^\dagger\hat{L}_m\rangle_c. \tag{6}$$

Here $\langle A\rangle\equiv \mathrm{Tr}\left[A\right]/d$ and $\langle AB\rangle_c\equiv\langle AB\rangle-\langle A\rangle\langle B\rangle$. d is the Hilbert space dimension of the Hamiltonian H.

2) The long-time behavior of this normalized SFF is a constant plateau whose value is given by

$$g(t\to\infty,\gamma\neq 0)=\frac{1}{d}. \tag{7}$$

Below, we give some simple arguments for these general properties. At the short-time limit, we can perform a Taylor expansion in t to the leading order:

$$\begin{aligned}\mathrm{Tr}[e^{-i(\hat{H}_s-i\hat{H}_d)t}] &= \mathrm{Tr}[1-i(\hat{H}_s-i\hat{H}_d)t]+O(t^2)\\ &\approx \mathrm{Tr}[e^{-i\hat{H}_s t}]\,\mathrm{Tr}[e^{-\hat{H}_d t}]/d.\end{aligned} \tag{8}$$

This leads to

$$F_\gamma(t)\simeq F(t,\beta=0)\frac{\mathrm{Tr}[e^{-\hat{H}_d t}]}{d}. \tag{9}$$

In the early-time regime, it is known that the correlation between the left and right systems in the doubled space is much smaller than the correlation within the same system [14], then we ignore the correlation contribution of the first term of the $\hat{H}_d$ in Eq. (3) when evaluating the last line of Eq. (9). Using the fact that the second and the third terms of the $\hat{H}_d$ commute with each other, we further obtain

$$F_\gamma(t)\simeq F(t,\beta=0)e^{-\sum_m 2\langle\hat{L}_m^\dagger\hat{L}_m\rangle_c\gamma t}. \tag{10}$$

This leads to the expression of α in Eq. (6), and its detailed derivation is in the supplementary materials [65]. As time increases, the correlation between the left and right contours generally increases, thus the assumption above is not valid at the intermediate time. Therefore, the normalized SFF generally does not have this exponential decay behavior at the intermediate time scales $\gamma t\sim 1$.

The final plateau value of the normalized SFF can be understood by investigating Eq. (4). Only the steady state with zero-imaginary eigenvalue will give a non-vanishing contribution to the long-time plateau value of SFF, and this gives the expression Eq. (7). In addition, if there are more than one steady state, then Eq. (7) should be changed to $g(t\to\infty,\gamma\neq 0)=\frac{\theta}{d}$. Here, θ is the total number of steady states.

Moreover, we can analyze the late-time regime using the effective field theory approach [11, 14]. The main idea is to approximate Green's functions on the path-integral contour of the SFF by their counterparts on a Keldysh contour with an auxiliary imaginary time separation between forward and backward evolutions. The SFF defined in Eq. (4) can be written as the path-integral

$$F_\gamma(t)=\int\mathcal{D}\Delta\mathcal{D}E_{\mathrm{aux}}e^{-S_{\mathrm{eff}}(\Delta,E_{\mathrm{aux}})}. \tag{11}$$

Without any dissipation, the linear ramp can be understood as an integration over the zero mode Δ and its conjugate variable E_{aux}. Δ describes the relative time shift between forward and backward evolution branches and E_{aux} can be understood as the energy of the system. In closed systems, there is no coupling between two branches, and the effective action $S^0_{\mathrm{eff}}(\Delta,E_{\mathrm{aux}})$ does not depend on Δ. Consequently, the integral over Δ from 0 to t leads to a linear slope. When the dissipation strength becomes small but finite, we find perturbatively

$$\delta S_{\mathrm{eff}}=-2\gamma t\sum_i G_{\mathrm{W},i}(\Delta,E_{\mathrm{aux}}). \tag{12}$$

Here $G_{\mathrm{W},i}(t,E_{\mathrm{aux}})$ is the Wightmann Green's function of operator $\hat{L}_i$ with energy E_{aux} [14]

$$G_{\mathrm{W},i}(\Delta,E_{\mathrm{aux}})=\langle e^{i\hat{H}\Delta}e^{-\frac{\beta_{\mathrm{aux}}}{2}\hat{H}}\hat{L}_i e^{-i\hat{H}\Delta}e^{-\frac{\beta_{\mathrm{aux}}}{2}\hat{H}}\hat{L}_i^\dagger\rangle_c, \tag{13}$$

where $\beta_{\mathrm{aux}}(E_{\mathrm{aux}})$ is determined by the thermodynamic relation. This leads to a finite mass for Δ, which increases linearly as time increases. In particular, as $t\to\infty$, the mode will be pinned at $\Delta=0$, which terminates the presence of the linear ramp. The role of different

types of Lindblad operators in shaping the general properties of the normalized SFF can also be discussed [66].

4 Examples

In the following, we use the SYK model, the random matrix model, and the Bose–Hubbard model as examples to illustrate these general properties of the normalized SFF in the open system.

We comment here that the SYK model and the random matrix model are both good examples to analytically calculate the SFF since they both involve random averages over different realizations that rattle the energy eigenvalues. The random average smooths out the fluctuations that come from the oscillating terms in the SFF, thus making it a smooth function of time. In comparison, the SFF has extensive spikes in the Bose–Hubbard model that come from the zeros of the SFF, and we need to do the time slice average to get a smooth SFF curve.

4.1 SYK model

We consider the SFF of the SYK model [67–71] whose Hamiltonian is of the form

$$\hat{H} = i^{\frac{q}{2}} \sum_{a_1<\ldots<a_q}^{N} J_{a_1,\ldots,a_q} \hat{\psi}_{a_1} \ldots \hat{\psi}_{a_q}. \tag{14}$$

Here, $J_{a_1,\ldots,a_q}$ is a random variable that satisfies the Gaussian distribution with mean zero and variance

$$\langle J_{a_1,\ldots,a_q} J_{a_1',\ldots,a_q'} \rangle = \delta_{a_1,a_1'} \ldots \delta_{a_q,a_q'} \frac{J^2(q-1)!}{N^{q-1}},$$

and $\hat{\psi}$ is the Majorana fermion operator. The Lindblad jump operators are chosen as the single Majorana Fermion operators.

We numerically compute the SFF for SYK model with $q = 4$ in Fig. 2, and there are several noteworthy features of this figure. First, we find that curves with different dissipation γ collapse well into a single line when they are plotted in terms of γt. Second, the early-time exponential decay in the SYK model is visible in Fig. 2, and it agrees well with our analytical result $e^{-N\gamma t}$ at early time region $\gamma t < 0.2$. Third, the long-time value of the SFF curve is a non-vanishing plateau whose value is $1/2^{N+1}$.

Furthermore, we can then write the SFF of the SYK model as a path-integral with the Lindblad operator chosen as the single Majorana fermion operator $\hat{L}_i = \hat{\psi}_i$. Also, the dissipation strength is chosen as the constant γ. We can then solve the early-time saddle-point solutions of the effective action, and to the first-order of dissipation strength γ, the effective action at the saddle point is

$$I[G, \Sigma] = I_0[G, \Sigma] + N\gamma T.$$

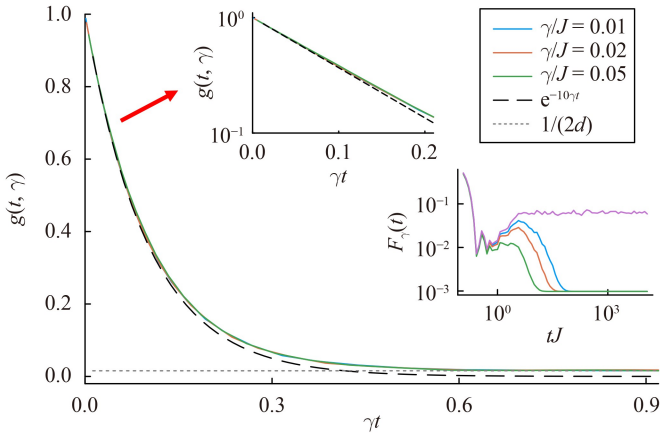

Fig. 2 The normalized SFF dynamics for SYK model with $q = 4$ as a function of γt. γ is the dissipation strength. The Lindblad jump operators are chosen as the single Majorana Fermion operators. The dashed line is a theoretical prediction of the initial slope based Eq. (6). The gray dot line is the prediction of the final plateau value. The left inset shows the early-time behavior of the normalized SFF. The right inset is a log–log plot of the SFF at different dissipation strengths, and the purple line is SFF without dissipation for comparison. The total number of Majorana Fermion is $N = 10$, and the random sample size is 200.

Thus, we obtain the normalized SFF as $g(t, \gamma) = \exp(-N\gamma T)$. It has an exponential decay behavior at the early time. The details of the derivation of the SFF in the SYK model are included in the supplementary [65]. A similar analysis of the SFF in the Brownian SYK is also included, in which the normalized SFF also has an early-time exponential decay behavior [65]. Moreover, since the spectrum of the Majorana SYK model with N mod 8 is not 0 has a 2-fold degeneracy [4, 72], the final plateau value of the normalized SFF is $\frac{1}{2d}$ instead of $\frac{1}{d}$ as shown in Fig. 2.

4.2 The random matrix theory

We now consider the SFF in Gaussian unitary ensemble (GUE). The SFF we defined in Eq. (4) can be written in RMT as

$$F_\gamma(t) = \frac{1}{N^2} \langle \mathrm{Tr}[e^{i\hat{H}^D t}] \rangle \tag{15}$$

with $\hat{H}^D = \hat{H}_s - i\hat{H}_d$ being a random matrix defined on doubled space. Here, $\hat{H}_s = \hat{H}_L \otimes \hat{\mathcal{I}}_R - \hat{\mathcal{I}}_L \otimes \hat{H}_R^T$ and $\hat{H}_d = \gamma(-2\hat{L}_L \otimes \hat{L}_R^* + (\hat{L}^\dagger \hat{L})_L \otimes \hat{\mathcal{I}}_R + \hat{\mathcal{I}}_L \otimes (\hat{L}^\dagger \hat{L})_R^*$ with $\hat{H}$ and L both are $N \times N$ random Hermitian matrices. The bracket $\langle \cdots \rangle$ means an averaging with respect to the Gaussian distribution:

$$P(H) = \frac{1}{\mathcal{Z}} e^{-\frac{N}{2}\mathrm{Tr}(\hat{H}^2)}, \quad P(L) = \frac{1}{\mathcal{Z}} e^{-\frac{N}{2}\mathrm{Tr}(L^2)}. \tag{16}$$

Then we consider the SFF in open systems in RMT.

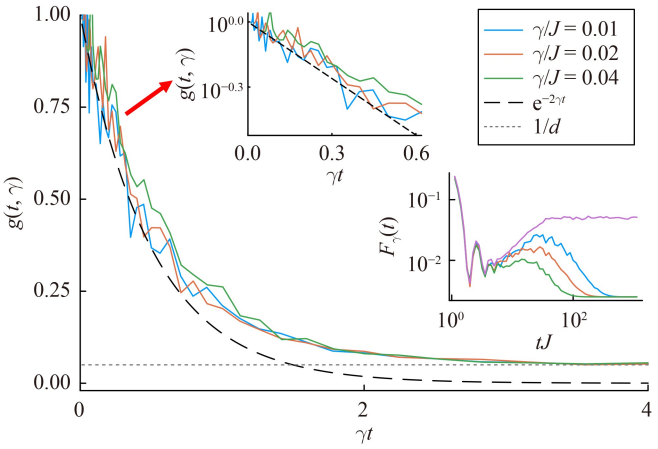

Fig. 3 The normalized SFF dynamics for GUE random matrices with dimension $N_{dim} = 20$ as a function of γt. γ is the dissipation strength. The Lindblad jump operators are chosen as the random hermitian matrix of GUE. The dashed line is a theoretical prediction of the initial slope based on Eq. (6). The gray dot line is the prediction of the final plateau value. The left inset shows the early-time behavior of the normalized SFF. The right inset is a log–log plot of the SFF as a function of tJ, and the purple line is SFF without dissipation for comparison. Here, the random realization of H and L is independent, and we randomize them each for 100 realizations.

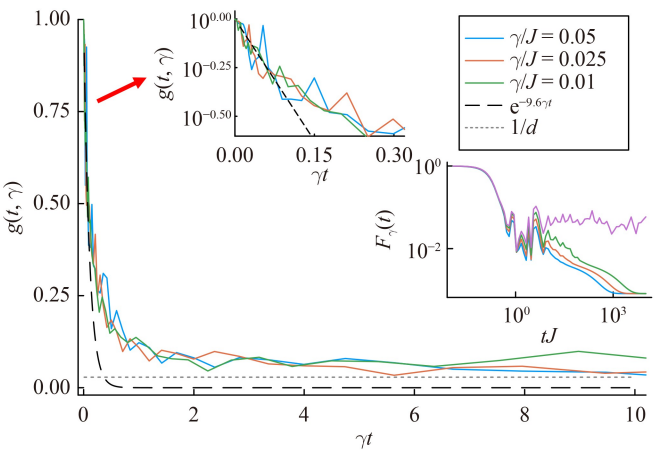

Fig. 4 The normalized SFF dynamics for 1D the Bose-Hubbard model as a function of γt. γ is the dissipation strength. The dashed line is a fitting of the initial slope based on Eq. (6). The gray dot line is the prediction of the final plateau value. The left inset shows the short-time behavior of the normalized SFF. The right inset is a log–log plot of the SFF as a function of tJ, and the purple line is SFF without dissipation for comparison. Here, $U/J = 3.128$ and the number of sites $N_s = 4$, and the number of bosons $N_b = 4$.

The SFF of open systems defined in Eq. (4) can be written as

$$F_\gamma(t) = \frac{\int \mathrm{d}H\mathrm{d}L \mathrm{e}^{-\frac{N}{2}\mathrm{Tr}H^2}\mathrm{e}^{-\frac{N}{2}\mathrm{Tr}L^2}\mathrm{Tr}\mathrm{e}^{-\mathrm{i}t\hat{H}^D}}{\int \mathrm{d}H\mathrm{d}L \mathrm{e}^{-\frac{N}{2}\mathrm{Tr}H^2}\mathrm{e}^{-\frac{N}{2}\mathrm{Tr}L^2}}. \tag{17}$$

In Fig. 3, we present $F_\gamma(t)$ for the GUE of matrices with dimension $N = 20$. We find that without dissipation the SFF first dips below its plateau value and then climb back up in a linear fashion (this region is also called the *ramp*), joining onto the plateau as depicted in the right inset of Fig. 3. Also, when we add a small dissipation, we find a similar dip-ramp behavior of the SFF, whereas it then decays to a plateau value that is lower than the case without dissipation. Moreover, the height of the plateau is of order $1/N$ without dissipation which is the mean level spacing, and the height of the plateau is of order $1/N^2$ with non-zero dissipation.

To understand this behavior of SFF with dissipation, we can directly calculate the normalized SFF, and the derivation details are included in the supplementary material [65]. We obtain the normalized SFF at early times

$$g(t,\gamma) \simeq \mathrm{e}^{-2\gamma t}, \gamma t \ll 1, \tag{18}$$

and this is an exponential decay behavior which is also visible in the numerical results in Fig. 3, and it is in good agreement with $\mathrm{e}^{-2\gamma t}$ at $\gamma t < 0.5$. On the other hand, in the long time limit $t \to \infty$, we find $g(t \to \infty, \gamma \neq 0) = \frac{1}{N}$, and $g(t \to \infty, \gamma = 0) = 1$. This explains the difference between the final plateau value in the case with and without dissipation as depicted in Fig. 3.

4.3 Bose–Hubbard model

We now consider the SFF of the 1D Bose–Hubbard model with dissipation. The Hamiltonian of the Bose–Hubbard model is

$$\hat{H} = -J\sum_{\langle i,j\rangle}\hat{b}_i^\dagger\hat{b}_j + \frac{U}{2}\sum_i \hat{n}_i(\hat{n}_i - 1). \tag{19}$$

Here, J is the strength of the nearest neighbor hopping, and U is the strength of the on-site interaction. In an open system, we set γ as a time-independent dissipation strength. Also, we set the Lindblad jump operators as $\hat{L}_m = \hat{n}_m$. Here $m = 1, 2, ..., N_s$, and N_s is the total number of sites.

The normalized SFF of the Bose–Hubbard model is illustrated in Fig. 4, and SFF is shown in the right inset. In our numerical simulation, we set $U/J = 3.128$ which is in the quantum critical region of 1D BHM [73]. Previous simulations suggest that the system exhibits quantum many-body chaos [74], although it is debatable that the system is most chaotic near the criticality [75, 76]. Meanwhile, since the SFF has extensive spikes in the Bose–Hubbard model, we perform the time slice average to get a smooth SFF curve in Fig. 4. This time average excludes possible non-general features, as discussed in

Refs. [61, 62] for closed systems. The number of time points that we average over is $N_{average} = 10$. The details of this average are added in the supplementary [65]. The initial exponential decay curve obtained by Eq. (6) is also included for comparison. The early-time exponential decay of the normalized SFF is visible in the left inset of Fig. 4, and it agrees well with the theoretical curve at $\gamma t < 0.15$.

5 Conclusion

In this letter, we have generalized the SFF to open quantum systems driven by the Lindblad master equation. We show that the normalized SFF of open systems generally has a dip-ramp structure and then decays to the plateau behavior at small dissipation strength. In particular, we unveil two general properties of the normalized SFF including the early-time exponential decay behavior determined by the Lindblad operators and the late-time plateau behavior that relates to the number of steady states. Our main tools are the SYK model, the random matrix model, and the Bose–Hubbard model. Using numerical techniques, we have obtained the behavior of SFF in these three models at all times. Then we are able to extract the general early-time and late-time behaviors of the normalized SFF, and we find good agreement between the numerics and analytical results.

Our work potentially opens up many interesting directions: firstly, the dynamics of the SFF of open systems have a close relationship with the Lindblad spectrum [77], and therefore the SFF can be used as a diagnosis of the structure of the Lindblad spectrum. Secondly, it will be interesting to study the intermediate time scales behavior of the SFF of the open system which might go through a phase transition and have some critical behaviors [54]. Thirdly, the SFF in open systems that we discussed here can be similarly measured in experiments [78–80] via generalization to the doubled space, and the detail is left to the appendix [65].

Meanwhile, the dynamical manifestations of level repulsion can be shown in the form of a drop in the value of the survival probability below its saturation point, which is known as the *correlation hole* [81–85]. Since the survival probability is the probability of finding the system in its initial state at a later time, this survival probability is the same as the SFF at inverse temperature β when the initial state is chosen as the coherent Gibbs state of inverse temperature β. Therefore, the dip-ramp behavior of the correlation hole has a close relation to the SFF. To generalize the study of survival probability in open quantum systems, we can replace the unitary evolution with an evolution governed by the Lindblad master equation. This results in an alternative definition of the SFF in open systems, which includes off-diagonal terms between eigenstates of the Hamiltonian, as discussed in the Electronic Supplementary Materials (Appendix A) [65]. Numerically, we verify that this new definition closely corresponds to the definition discussed in the main text for nearly the entire time regime. Consequently, we anticipate that the investigation of correlation holes can also be extended to open systems. A comprehensive study of this extension, however, will be postponed in future works.

Moreover, the Lindbladian description of open systems relies on the Markovian approximation of the environment. Consequently, time scales that exceed the Markovian approximation may not be accurately described by the Lindblad master equation. For open systems that reach their steady state within a time scale shorter than this Markovian approximation time scale, this is typically not a significant challenge. However, it is possible that in certain specific many-body systems, the steady state is not achieved within the time frame of the Markovian approximation. In such cases, our analysis of the long-time plateau behavior, which is related to the Lindblad operators, may not be entirely reliable as the Lindblad description is not suitable in this regime.

The Lindblad equation requires the Markovian–Born approximation and the secular approximation on the interaction term [86]. Building on previous studies of the Markovian approximation, for times $t > 1/\omega_d$, where ω_d represents the width of the bath system correlation spectrum, the Markovian approximation becomes applicable [87]. The Markovian approximation provides a description on a coarse-grained time scale with the assumption that environmental excitations decay over times that are not resolved. However, if the time duration is too long, environmental excitations will influence the original system, and this characteristic time scale depends on the relative degrees of freedom, temperature, and the detailed spectrum shape of the bath. Therefore, comparing the Heisenberg time and the failure time of the Markovian approximation is a specific problem that varies with different settings. Therefore, it is important to emphasize that the generality we have discussed in our paper is applicable within the time domain where the Markovian treatment of the environment holds. Time scales exceeding this domain require further exploration, and we leave this for future studies

Declarations The authors declare that they have no competing interests and there are no conflicts.

Electronic supplementary materials The online version contains supplementary material available at https://doi.org/10.1007/s11467-024-1406-7 and https://journal.hep.com.cn/fop/EN/10.1007/s11467-024-1406-7.

Acknowledgements We thank Hui Zhai for the invaluable discussions and for carefully reading the manuscript. We thank Yingfei Gu, Haifeng Tang, Liang Mao, and Hanteng Wang for the helpful discus-

sions. We especially thank Adolfo del Campo for assisting us in rectifying our estimation of the decay exponent in the early-time regime and for bringing to our attention several relevant papers that were overlooked in a previous version.

References and notes

1. E. Brézin and A. Zee, Universality of the correlations between eigenvalues of large random matrices, *Nucl. Phys. B* 402(3), 613 (1993)
2. E. Brézin and S. Hikami, Correlations of nearby levels induced by a random potential, *Nucl. Phys. B* 479(3), 697 (1996)
3. S. Müller, S. Heusler, P. Braun, F. Haake, and A. Altland, Periodic-orbit theory of universality in quantum chaos, *Phys. Rev. E* 72(4), 046207 (2005)
4. J. S. Cotler, G. Gur-Ari, M. Hanada, J. Polchinski, P. Saad, S. H. Shenker, D. Stanford, A. Streicher, and M. Tezuka, Black holes and random matrices, *J. High Energy Phys.* 2017(5), 118 (2017)
5. J. Liu, Spectral form factors and late time quantum chaos, *Phys. Rev. D* 98(8), 086026 (2018)
6. P. Kos, M. Ljubotina, and T. Prosen, Many-body quantum chaos: Analytic connection to random matrix theory, *Phys. Rev. X* 8(2), 021062 (2018)
7. B. Bertini, P. Kos, and T. Prosen, Exact spectral form factor in a minimal model of many-body quantum chaos, *Phys. Rev. Lett.* 121(26), 264101 (2018)
8. A. Chan, A. De Luca, and J. T. Chalker, Spectral statistics in spatially extended chaotic quantum many-body systems, *Phys. Rev. Lett.* 121(6), 060601 (2018)
9. J. Kudler-Flam, L. Nie, and S. Ryu, Conformal field theory and the web of quantum chaos diagnostics, *J. High Energy Phys.* 2020(1), 175 (2020)
10. D. Roy and T. Prosen, Random matrix spectral form factor in kicked interacting fermionic chains, *Phys. Rev. E* 102(6), 060202 (2020)
11. M. Winer and B. Swingle, Hydrodynamic theory of the connected spectral form factor, *Phys. Rev. X* 12(2), 021009 (2022)
12. D. Roy, D. Mishra, and T. Prosen, Spectral form factor in a minimal bosonic model of many-body quantum chaos, *Phys. Rev. E* 106(2), 024208 (2022)
13. R. Barney, M. Winer, C. L. Baldwin, B. Swingle, and V. Galitski, Spectral statistics of a minimal quantum glass model, *SciPost Phys.* 15, 084 (2023)
14. P. Saad, S. H. Shenker, and D. Stanford, A semi-classical ramp in SYK and in gravity, arXiv: 1806.06840 (2018)
15. H. Gharibyan, M. Hanada, S. H. Shenker, and M. Tezuka, Onset of random matrix behavior in scrambling systems, *J. High Energy Phys.* 2018(7), 124 (2018)
16. M. Winer, S. K. Jian, and B. Swingle, Exponential ramp in the quadratic Sachdev–Ye–Kitaev model, *Phys. Rev. Lett.* 125(25), 250602 (2020)
17. R. Shir, P. Martinez-Azcona, and A. Chenu, Full range spectral correlations and their spectral form factors in chaotic and integrable models, arXiv: 2311.09292 (2023)
18. Y. N. Zhou, L. Mao, and H. Zhai, Rényi entropy dynamics and Lindblad spectrum for open quantum systems, *Phys. Rev. Res.* 3(4), 043060 (2021)
19. G. Mazzucchi, W. Kozlowski, S. F. Caballero-Benitez, T. J. Elliott, and I. B. Mekhov, Quantum measurement-induced dynamics of many-body ultracold bosonic and fermionic systems in optical lattices, *Phys. Rev. A* 93(2), 023632 (2016)
20. Y. Li, X. Chen, and M. P. A. Fisher, Quantum Zeno effect and the many-body entanglement transition, *Phys. Rev. B* 98(20), 205136 (2018)
21. B. Skinner, J. Ruhman, and A. Nahum, Measurement-induced phase transitions in the dynamics of entanglement, *Phys. Rev. X* 9(3), 031009 (2019)
22. Y. Li, X. Chen, and M. P. A. Fisher, Measurement-driven entanglement transition in hybrid quantum circuits, *Phys. Rev. B* 100(13), 134306 (2019)
23. M. Szyniszewski, A. Romito, and H. Schomerus, Entanglement transition from variable-strength weak measurements, *Phys. Rev. B* 100(6), 064204 (2019)
24. A. Chan, R. M. Nandkishore, M. Pretko, and G. Smith, Unitary-projective entanglement dynamics, *Phys. Rev. B* 99(22), 224307 (2019)
25. R. Vasseur, A. C. Potter, Y. Z. You, and A. W. W. Ludwig, Entanglement transitions from holographic random tensor networks, *Phys. Rev. B* 100(13), 134203 (2019)
26. T. Zhou and A. Nahum, Emergent statistical mechanics of entanglement in random unitary circuits, *Phys. Rev. B* 99(17), 174205 (2019)
27. M. J. Gullans and D. A. Huse, Scalable probes of measurement-induced criticality, *Phys. Rev. Lett.* 125(7), 070606 (2020)
28. C. M. Jian, Y. Z. You, R. Vasseur, and A. W. W. Ludwig, Measurement-induced criticality in random quantum circuits, *Phys. Rev. B* 101(10), 104302 (2020)
29. Y. Fuji and Y. Ashida, Measurement-induced quantum criticality under continuous monitoring, *Phys. Rev. B* 102(5), 054302 (2020)
30. A. Zabalo, M. J. Gullans, J. H. Wilson, S. Gopalakrishnan, D. A. Huse, and J. H. Pixley, Critical properties of the measurement-induced transition in random quantum circuits, *Phys. Rev. B* 101(6), 060301 (2020)
31. M. J. Gullans and D. A. Huse, Dynamical purification phase transition induced by quantum measurements, *Phys. Rev. X* 10(4), 041020 (2020)
32. S. Choi, Y. Bao, X. L. Qi, and E. Altman, Quantum error correction in scrambling dynamics and measurement-induced phase transition, *Phys. Rev. Lett.* 125(3), 030505 (2020)
33. Y. Bao, S. Choi, and E. Altman, Theory of the phase transition in random unitary circuits with measurements, *Phys. Rev. B* 101(10), 104301 (2020)
34. A. Nahum, S. Roy, B. Skinner, and J. Ruhman, Measurement and entanglement phase transitions in all-to-all quantum circuits, on quantum trees, and in Landau–Ginsburg theory, *PRX Quantum* 2(1), 010352 (2021)
35. R. Fan, S. Vijay, A. Vishwanath, and Y. Z. You, Self-organized error correction in random unitary circuits with measurement, *Phys. Rev. B* 103(17), 174309 (2021)
36. S. Sang and T. H. Hsieh, Measurement-protected quantum phases, *Phys. Rev. Res.* 3(2), 023200 (2021)

37. O. Alberton, M. Buchhold, and S. Diehl, Entanglement transition in a monitored free-fermion chain: From extended criticality to area law, *Phys. Rev. Lett.* 126(17), 170602 (2021)
38. A. Lavasani, Y. Alavirad, and M. Barkeshli, Measurement-induced topological entanglement transitions in symmetric random quantum circuits, *Nat. Phys.* 17(3), 342 (2021)
39. X. Turkeshi, A. Biella, R. Fazio, M. Dalmonte, and M. Schiró, Measurement-induced entanglement transitions in the quantum Ising chain: From infinite to zero clicks, *Phys. Rev. B* 103(22), 224210 (2021)
40. Y. Le Gal, X. Turkeshi, and M. Schiró, Volume-to-area law entanglement transition in a non-Hermitian free fermionic Chain, *SciPost Phys.* 14, 138 (2023)
41. S. K. Jian, C. Liu, X. Chen, B. Swingle, and P. Zhang, Measurement-induced phase transition in the monitored Sachdev–Ye–Kitaev model, *Phys. Rev. Lett.* 127(14), 140601 (2021)
42. P. Zhang, C. Liu, S. K. Jian, and X. Chen, Universal entanglement transitions of free fermions with long-range non-unitary dynamics, *Quantum* 6, 723 (2022)
43. C. Liu, P. Zhang, and X. Chen, Non-unitary dynamics of Sachdev–Ye–Kitaev chain, *SciPost Phys.* 10, 048 (2021)
44. P. Zhang, S. K. Jian, C. Liu, and X. Chen, Emergent replica conformal symmetry in non-Hermitian SYK2 chains, *Quantum* 5, 579 (2021)
45. P. Zhang, Quantum entanglement in the Sachdev–Ye–Kitaev model and its generalizations, *Front. Phys.* 17(4), 43201 (2022)
46. S. Sahu, S. K. Jian, G. Bentsen, and B. Swingle, Entanglement phases in large-n hybrid Brownian circuits with long-range couplings, *Phys. Rev. B* 106(22), 224305 (2022)
47. C. Liu, H. Tang, and H. Zhai, Krylov complexity in open quantum systems, *Phys. Rev. Res.* 5, 033085 (2023)
48. A. Bhattacharya, P. Nandy, P. P. Nath, and H. Sahu, Operator growth and Krylov construction in dissipative open quantum systems, *J. High Energy Phys.* 2022(12), 81 (2022)
49. B. Bhattacharjee, X. Cao, P. Nandy, and T. Pathak, Operator growth in open quantum systems: Lessons from the dissipative SYK, *J. High Energy Phys.* 2023(3), 54 (2023)
50. A. Bhattacharya, P. Nandy, P. P. Nath, and H. Sahu, On Krylov complexity in open systems: An approach via bi-Lanczos algorithm, *J. High Energy Phys.* 2023, 66 (2023)
51. T. Can, Random Lindblad dynamics, *J. Phys. A Math. Theor.* 52(48), 485302 (2019)
52. J. Li, T. Prosen, and A. Chan, Spectral statistics of non-Hermitian matrices and dissipative quantum chaos, *Phys. Rev. Lett.* 127(17), 170602 (2021)
53. P. Kos, B. Bertini, and T. Prosen, Chaos and ergodicity in extended quantum systems with noisy driving, *Phys. Rev. Lett.* 126(19), 190601 (2021)
54. K. Kawabata, A. Kulkarni, J. Li, T. Numasawa, and S. Ryu, Dynamical quantum phase transitions in SYK Lindbladians, *Phys. Rev. B* 108, 075110 (2023)
55. Z. Xu, A. Chenu, T. Prosen, and A. del Campo, Thermofield dynamics: Quantum chaos versus decoherence, *Phys. Rev. B* 103(6), 064309 (2021)
56. J. Cornelius, Z. Xu, A. Saxena, A. Chenu, and A. del Campo, Spectral filtering induced by non-Hermitian evolution with balanced gain and loss: Enhancing quantum chaos, *Phys. Rev. Lett.* 128(19), 190402 (2022)
57. A. S. Matsoukas-Roubeas, F. Roccati, J. Cornelius, Z. Xu, A. Chenu, and A. del Campo, Non-Hermitian Hamiltonian deformations in quantum mechanics, *J. High Energy Phys.* 2023(1), 60 (2023)
58. F. Roccati, F. Balducci, R. Shir, and A. Chenu, Diagnosing non-Hermitian many-body localization and quantum chaos via singular value decomposition, arXiv: 2311.16229 (2023)
59. If we simply generalize the definition of the SFF for non-Hermitian systems as follows: $F_\gamma(t) = \frac{1}{[\mathcal{Z}(0)]^2}\sum_{m,n} \mathrm{e}^{-\mathrm{i}(\epsilon_m-\epsilon_n)t}$. where $\{\epsilon_n\}$ is the set of eigenvalues of the non-Hermitian system, and we denote the real and imaginary parts of the eigenvalues as α_n and β_n respectively. Since the energy eigenvalues of a general non-Hermitian system are complex, implying that the imaginary part β_n is generally nonzero, from the definition we observe that $F_\gamma(t) = \frac{1}{[\mathcal{Z}(0)]^2}\sum_{m,n} \mathrm{e}^{-\mathrm{i}(\alpha_m-\alpha_n)t}\mathrm{e}^{(\beta_m-\beta_n)t}$. Hence, for the set of m, n that satisfies $\beta_m - \beta_n > 0$, there will be an exponential growth term $\mathrm{e}^{(\beta_m-\beta_n)t}$ in the above definition, resulting in the exponential growth of the SFF as time increases.
60. P. Martinez-Azcona and A. Chenu, Analyticity constraints bound the decay of the spectral form factor, *Quantum* 6, 852 (2022)
61. O. Agam, B. L. Altshuler, and A. V. Andreev, Spectral statistics: From disordered to chaotic systems, *Phys. Rev. Lett.* 75(24), 4389 (1995)
62. E. B. Bogomolny and J. P. Keating, Gutzwiller's trace formula and spectral statistics: Beyond the diagonal approximation, *Phys. Rev. Lett.* 77(8), 1472 (1996)
63. J. E. Tyson, Operator-Schmidt decompositions and the Fourier transform, with applications to the operator-Schmidt numbers of unitaries, *J. Phys. Math. Gen.* 36(39), 10101 (2003)
64. M. Zwolak and G. Vidal, Mixed-state dynamics in one-dimensional quantum lattice systems: A time-dependent superoperator renormalization algorithm, *Phys. Rev. Lett.* 93(20), 207205 (2004)
65. In this supplementary, we show (A) alternative definitions of SFF; (B) the derivation of the pre-factor α in early decay region; (C, D, E) detailed calculation of SFF in three examples; (F) possible experimental realization of SFF.
66. In general, we think the types of different Lindblad operators will not change the general properties of the normalized SFF regarding its short-time exponential decay and long-time plateau behavior. Since the argument we provide just below Eq. (9) does not resume some specific form of the Lindblad operators. Nevertheless, different Lindblad operators may lead to a different number of steady states, thereby altering the value of θ. For example, let us consider a Hamiltonian H with charge conservation, such as our Bose–Hubbard model. In the main text, we focus on Lindblad operators that

preserve the particle number, ensuring that charge conservation is a strong $U(1)$ symmetry of the open system. In this scenario, there is at least one steady state in each charge sector, resulting in at least $N+1$ steady states in the full Fock space with arbitrary particle numbers. (Note that our discussions in the main text focus on a single charge sector.) In contrast, when some Lindblad operators couple different charge sectors, the system exhibits only a weak $U(1)$ symmetry. Consequently, there may be only one steady state even in the full Fock space.

67. P. Saad, S. H. Shenker, and D. Stanford, A semiclassical ramp in SYK and in gravity, arXiv: 1806.06840 (2018)
68. L. Sá, P. Ribeiro, and T. Prosen, Lindbladian dissipation of strongly-correlated quantum matter, *Phys. Rev. Res.* 4(2), L022068 (2022)
69. A. M. García-García, L. Sá, J. J. M. Verbaarschot, and J. P. Zheng, Keldysh wormholes and anomalous relaxation in the dissipative Sachdev–Ye–Kitaev model, *Phys. Rev. D* 107(10), 106006 (2023)
70. K. Kawabata, A. Kulkarni, J. Li, T. Numasawa, and S. Ryu, Dynamical quantum phase transitions in Sachdev–Ye–Kitaev Lindbladians, *Phys. Rev. B* 108(7), 075110 (2023)
71. H. Wang, C. Liu, P. Zhang, and A. M. García-García, Entanglement transition and replica wormholes in the dissipative Sachdev–Ye–Kitaev model, *Phys. Rev. D* 109(4), 046005 (2024)
72. Y. Z. You, A. W. W. Ludwig, and C. Xu, Sachdev–Ye–Kitaev model and thermalization on the boundary of many-body localized fermionic symmetry-protected topological states, *Phys. Rev. B* 95(11), 115150 (2017)
73. I. Danshita and A. Polkovnikov, Superfluid-to-Mott-insulator transition in the one-dimensional Bose–Hubbard model for arbitrary integer filling factors, *Phys. Rev. A* 84(6), 063637 (2011)
74. H. Shen, P. Zhang, R. Fan, and H. Zhai, Out-of-time-order correlation at a quantum phase transition, *Phys. Rev. B* 96(5), 054503 (2017)
75. I. Boettcher, P. Bienias, R. Belyansky, A. J. Kollár, and A. V. Gorshkov, Quantum simulation of hyperbolic space with circuit quantum electrodynamics: From graphs to geometry, *Phys. Rev. A* 102(3), 032208 (2020)
76. L. Pausch, A. Buchleitner, E. G. Carnio, and A. Rodríguez, Optimal route to quantum chaos in the Bose–Hubbard model, *J. Phys. A Math. Theor.* 55(32), 324002 (2022)
77. S. Denisov, T. Laptyeva, W. Tarnowski, D. Chruscinski, and K. Zyczkowski, Universal spectra of random Linblad operators, *Phys. Rev. Lett.* 123(14), 140403 (2019)
78. D. Poulin, R. Laflamme, G. J. Milburn, and J. P. Paz, Testing integrability with a single bit of quantum information, *Phys. Rev. A* 68(2), 022302 (2003)
79. D. V. Vasilyev, A. Grankin, M. A. Baranov, L. M. Sieberer, and P. Zoller, Monitoring quantum simulators via quantum nondemolition couplings to atomic clock qubits, *PRX Quantum* 1(2), 020302 (2020)
80. L. K. Joshi, A. Elben, A. Vikram, B. Vermersch, V. Galitski, and P. Zoller, Probing many-body quantum chaos with quantum simulators, *Phys. Rev. X* 12(1), 011018 (2022)
81. L. Leviandier, M. Lombardi, R. Jost, and J. P. Pique, A tool to measure statistical level properties in very complex spectra, *Phys. Rev. Lett.* 56(23), 2449 (1986)
82. J. P. Pique, Y. Chen, R. W. Field, and J. L. Kinsey, Chaos and dynamics on 0.5–300 ps time scales in vibrationally excited acetylene: Fourier transform of stimulated-emission pumping spectrum, *Phys. Rev. Lett.* 58(5), 475 (1987)
83. T. Guhr and H. A. Weidenmuller, Correlations in anticrossing spectra and scattering theory: Analytical aspects, *Chem. Phys.* 146(1–2), 21 (1990)
84. M. Lombardi and T. H. Seligman, Universal and nonuniversal statistical properties of levels and intensities for chaotic Rydberg molecules, *Phys. Rev. A* 47(5), 3571 (1993)
85. E. J. Torres-Herrera and L. F. Santos, Dynamical manifestations of quantum chaos: Correlation hole and bulge, *Philos. Trans. Royal Soc. A* 375(2108), 20160434 (2017)
86. H. P. Breuer and F. Petruccione, The Theory of Open Quantum Systems, Oxford University Press, Oxford, 2007
87. Y. C. Cheng and R. J. Silbey, Markovian approximation in the relaxation of open quantum systems, *J. Phys. Chem. B* 109, 21399 (2005)